

# Parameter identification for realistic pile-soil interaction analysis

M. S. A. Siddiquee, Salek M. Seraj & M. Shafiqul Bari  
 Bangladesh University of Engineering and Technology Dhaka, Bangladesh

Property	Symbol	Value	Unit
Soil type		Clay	
Soil strength	$c$	10.0	kN/m <sup>2</sup>
Soil friction angle	$\phi$	23	degrees
Soil modulus	$E_s$	10000	kN/m <sup>2</sup>
Soil Poisson's ratio	$\nu$	0.3	
Soil permeability	$k_x, k_y$	1.5	m/d
Soil unit weight	$\gamma$	18	kN/m <sup>3</sup>

**ABSTRACT:** The configuration of mesh parameters has considerable influence on the subsequent predictions of any finite element analysis pertaining to soil-structure interaction study. Ideally, infinitely extending fine mesh is expected to give accurate predictions when compared with coarser as well as not too extended mesh. However, increase in computation time and the very little improvement achieved due to this refinement make such an exercise less attractive. In the present paper, an extensive comparative study on mesh configuration, with respect to deep (pile) foundation, has been presented in order to arrive at a more objective mesh configuration as applicable to Dhaka soil. Modified Cam-Clay (MCC) model has been used in the study.

## 1 INTRODUCTION

In this study, seven very crucial parameters are identified (see Fig. 1). The parameters are, the radial extent of mesh from the pile edge ( $C_1$ ); the vertical extent of mesh from pile tip ( $C_2$ ); the rate of change of element size with horizontal distance from pile edge and vertical distance from pile tip ( $m_r$ ), the loading rate ( $L_i$ ); the number of elements along the pile length and its interface with soil ( $N_1$ ); the number of elements within a distance of twice the diameter of pile from pile tip ( $N_2$ ) and the thickness of interface element ( $T_i$ ).

The pile used in this study has a length of 19.3 m and diameter of 0.504 m. The various relevant soil and pile material parameters for this pile (Pile A) have been listed in Tables 1, 2, 3, 4, 5 and in Fig. 1.

## 2 MATERIAL PROPERTIES

In this study, the soil profile consists of two different layers, one is clay and the other is sand below it. Altogether six different material types are used in this study. Details of these material zones along with their respective properties are available in Bari (1996). Clay above the water table has been considered to be a separate layer and the clay layer has been set to obey Modified Cam-Clay model (MCC) while the sand layer is analyzed as elastic-perfectly-plastic model with modulus of elasticity increasing with depth. The frictional constant  $M$  is obtained from triaxial test (drained or undrained

with pore pressure measurement) on isotropically consolidated samples. The value of  $\phi'$  are 23° and 25° respectively (Kamal Uddin, 1990). Here, the permeability in both x and y direction are obtained from the research carried out by Siddiquee and Safiullah (1995) assuming that  $K_x = 1.5 K_y$ .

Since the laboratory values of modulus of elasticity of sand,  $E_s$ , although expensive to obtain, do not represent *in-situ* conditions well, SPT and

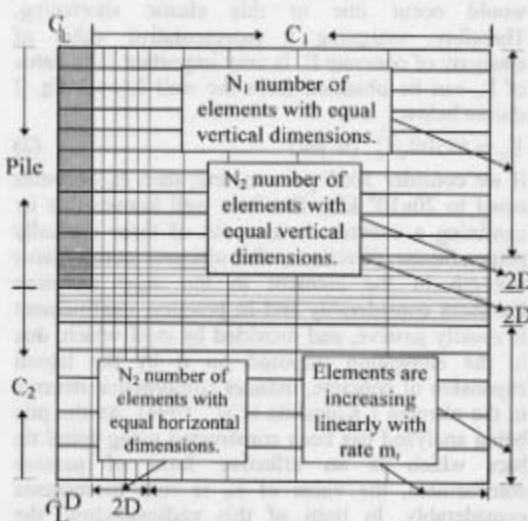


Fig. 1 Various critical mesh configuration parameters.

CPT values are widely used to obtain  $E_s$ . In the original study of Bari (1996), usually Eq. 1 has been used to calculate values of  $E_s$  and sometimes engineering judgement has been applied to arrive at representative input values.

$$E_s = (15200 \text{ to } 22000) \ln N' \quad (\text{kPa}) \quad (1)$$

### 2.1 Interface Parameters

For interface material properties, the parameters that are to be assigned are  $C_a$ ,  $\phi_a$ ,  $K_n$ ,  $G_s$  and  $G_{res}$ . The  $C_a$  and  $\phi_a$  values of interface element should be the  $C$  and  $\phi$  values respectively for pile and soil interface; not for soil itself. Thus,  $C_a$  is the adhesion between pile and soil while  $\phi_a$  is the angle of friction between pile and soil. For bored concrete piles, the value of  $\phi_a$  can be set to equal to  $\phi$ . Thus, in this study  $\phi_a$  values are set to be equal to  $\phi$  for respective soil type.

The value of  $G_s$  for interface can be obtained from shear test conducted between two dissimilar materials. As this is rather expensive, in this study the value of  $G_s$  has been assumed using a very high value of  $\nu$  as recommended by Bari (1996). The residual shear modulus, after the interface element has reached its limiting shear value ( $G_{res}$ ), should have a very low value as it is almost equal to zero in reality. So, in this study,  $G_{res}$  has been assigned to be equal to  $10 \text{ kN/m}^2$  arbitrarily to avert the numerical problems which may take place if such a value is set to zero.

### 2.2 Pile Material

A significant difference in displacement values would occur due to this elastic shortening. Therefore, assigning a representative value of elasticity of concrete  $E_c$  is very important. The value of  $E_c$  can be obtained from the well known Eq. 2 shown below.

$$E_c = 57500 \sqrt{f'_c} \quad (\text{in psi}) \quad (2)$$

If we consider 3000 psi concrete, then  $E_c$  becomes equal to  $20 \times 10^6 \text{ kPa}$ . But it is well known that by confining a concrete in two out of three mutually perpendicular directions, the ultimate compressive strength of the element in the third direction increases considerably and in practice, confinement is usually passive, and provided by steel which, due to the elongation imposed on it by the lateral expansion of concrete, induces compressive stresses in the element (Kinoshita et al., 1994). As the pile being analyzed has been constructed using spiral tie bars which is an effective form of passive confinement, the value of  $E_c$  is sure to increase considerably. In light of this understanding, the value of  $E_c$  has been used, although still underestimated, as  $30 \times 10^6 \text{ kPa}$  for 3000 psi concrete.

Tables 1, 2, 3 and 4 represent all the material properties used for pile A in this model in the light of previous discussions.

Table 1. Soil parameters for Clay layer (Pile A,  $\kappa = 0.01875$ ,  $\lambda = 0.075$ ,  $M = 0.898$ ,  $\nu = 0.25$ ).

Depth (m)	Soil Type	$e_{cs}$	$\gamma_{bulk}$ ( $\text{kN/m}^3$ )	$K_x$ (m/s)	$K_y$ (m/s)
0-3.3	Clay>W.T	0.81	13.5	8.E-10	5.3E-10
3.3-8.3	Clay<W.T.	0.81	19.0	8.E-10	5.3E-10

Table 2. Soil parameters for Sand layer (Pile A,  $\nu = 0.25$ ,  $C = 0$ ,  $\phi = 31^\circ$ ,  $E_0 = 50E3 \text{ kN/m}^2$ ).

Depth (m)	$\gamma_o$ (m)	$\gamma_{bulk}$ ( $\text{kN/m}^3$ )	$K_x$ (m/s)	$K_y$ (m/s)	Rate $m_1$ ( $\text{kN/m}^2/\text{m}$ )
8.33-34.3	28.3	19.5	5.E-4	3.E-4	2.E3

Table 3. Interface element parameters (Pile A,  $G_{res} = 10 \text{ kN/m}^2$ ).

Depth (m)	$C$ ( $\text{kN/m}^2$ )	$\phi$ (deg)	$K_n$ ( $\text{kN/m}^2$ )	$G_s$ ( $\text{kN/m}^2$ )
0-8.33	5	23	23.34 E4	1.01 E4
8.33-19.3	0	31	54.90 E4	2.1 E4

Table 4. Parameters for Pile Material.

	$E$ ( $\text{kN/m}^2$ )	$\nu$	$\gamma_{bulk}$ ( $\text{kN/m}^3$ )
Pile A	30 E6	0.20	23.5

Table 5. *In-situ* Stresses for different layers of Pile A.

Depth (m)	$\sigma_v'$ ( $\text{kN/m}^2$ )	$\sigma_h'$ ( $\text{kN/m}^2$ )	$U_o$ ( $\text{kN/m}^2$ )	$p_c'$ ( $\text{kN/m}^2$ )
0-3.3	44.55	27.143	0.0	44.35
3.3-8.3	89.55	54.56	50.0	89.145
8.3-34.3	336.55	163.215	310.0	0.0

## 3 FE DETAILS

In this study, 8-noded linear strain quadrilateral element with displacements unknown has been used for both pile elements and soil elements. For interface elements, the 6 noded interface element with displacement unknown is used. Axisymmetric analysis has been performed.

The positioning of interface elements along pile shaft specially near the tip calls for a special treatment. All along the pile shaft, the interface elements are rectangular having the longer dimension along the pile. But at the tip of pile the interface elements are set to be trapezoidal. This has been done to avoid the placement of one vertex of

interface element on the side of the soil element below where is no node present. If a node is placed at that point, then the aspect ratio of all soil elements below would be too large for accurate analysis.

#### 4 OPTIMUM MESH CONFIGURATION

The optimum mesh configuration is sought by varying the proposed parameters of the mesh one by one and finding out their meaningful range. In this way effective range of all parameters can be established. Determination of each factor is described in detail in the following sections.

##### 4.1 Determination of $C_1$

To investigate the effect of the variation of  $C_1$  on the accuracy of analysis, other parameters have to be kept unchanged. Table 6 shows the values of various parameters used in this study for determining  $C_1$ .

Table 6. Parameters used in fixing  $C_1$

$m_r$ (m/element)	$C_1$ (m)	$C_2$ (m)	$L_1$	$N_1$	$N_2$	$T_1$ (m)
0.25	5,10					
0.5	15,20	12	$L_1$	20	2	0.05
1	25,30					

Firstly, the effect of variation of  $C_1$  in the load-displacement curve is investigated which is shown in Fig. 2. It shows that for all values of  $C_1$  other than for  $C_1$  equal to 5 m and 10 m, the load-displacement curves have very insignificant or no difference. A value of 15 m for  $C_1$  may be considered to be an acceptable value for predictions without impairing accuracy.

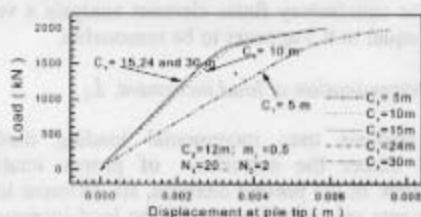


Fig. 2 Load-displacement curves for various radial extent of mesh.

Since the radial boundary of a mesh needs to be extended up to a point where stress caused by load on pile top become negligible, stress-norm  $\sigma_{sn}$  which represents the overall stress conditions of any element has been introduced as in Eq. 2.

$$(\sigma_{sn})_i = \sqrt{(\sigma_x)^2 + (\sigma_y)^2 + (\sigma_z)^2 + (\tau_{xy})^2} \quad (3)$$

Where,

$(\sigma_{sn})_i$  = stress-norm of element  $i$ ,  $\sigma_x$ ,  $\sigma_y$  and  $\sigma_z$  = normal stress of element  $i$  in  $x$ ,  $y$  and  $z$  directions caused by extra load on pile top only, and  $\tau_{xy}$  = shear stress of element  $i$  in  $xy$  plane caused by extra load on pile top only. All the stresses have been calculated by subtracting the corresponding stress caused by *in-situ* stress only from the stress caused by load and *in-situ* stress combined.

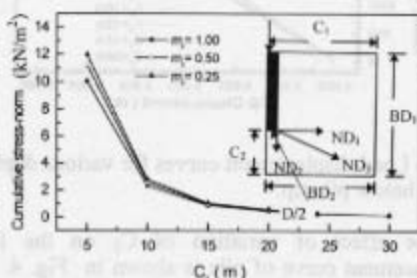


Fig. 3 Variation of cumulative stress-norm along boundary  $BD_1$  with radial distance from pile.

The  $\sigma_{sn}$  for every element along the boundary 1 ( $BD_1$ ), as shown in Fig. 3, has been calculated. These stress-norms for each element along  $BD_1$  is then summed up to have  $\sum(\sigma_{sn})_i$ . Now, this  $\sum(\sigma_{sn})_i$  for each value of  $C_1$  is calculated and plotted in Fig. 3 for various values of  $m_r$ . It can be seen from Fig. 3 that  $\sum(\sigma_{sn})_i$  for all elements along  $BD_1$  decreases with increasing values of  $C_1$ . It is also clear that for all values of  $m_r$  analyzed, the trend is similar and all curves converge as  $C_1$  takes larger values. Starting from a value as high as more than 10  $kN/m^2$ ,  $\sum(\sigma_{sn})_i$  reaches a value as low as below 0.4  $kN/m^2$ . For  $C_1$  ranging from 5 to 15 m, the value of  $\sum(\sigma_{sn})_i$  decreases sharply, but after that decreases very slowly with increasing  $C_1$ . Therefore, the convergence of load-displacement curves for  $C_1$  equal to 15 m or greater (Fig. 2) is justified as the values of  $\sum(\sigma_{sn})_i$  for them are very insignificant. Although  $C_1$  equal to 15 m gives reasonable results,  $C_1$  equal to 20 m has been selected in this study as the radial distance upto which the mesh should be extended in order to mimic the soil-structure system more faithfully.

##### 4.2 Determination of $C_2$

A comparative analysis, similar to the one undertaken for  $C_1$ , has been performed in order to fix

$C_2$ . The parameters used in this exercise are presented in Table 7.

Table 7. Parameters used in analysis for fixing  $C_2$

$m_r$ (m/element)	$C_1$ (m)	$C_2$ (m)	$L_i$	$N_1$	$N_2$	$T_1$ (m)
0.25		5,10				
0.5	20	15,20	$L_1$	20	2	0.05
1		25,30				

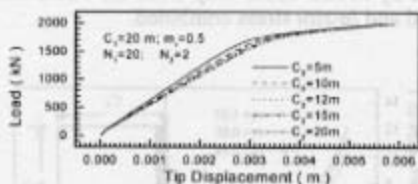


Fig. 4 Load-displacement curves for various depth of mesh below pile tip.

The effect of variation of  $C_2$  on the load-displacement curve of pile is shown in Fig. 4. The figure shows that for increasing values of  $C_2$ , the curves tend to shift rightwards slightly. At the region, where transition from linear state to nonlinear state occurs, the rightward shifts are most significant. After that region, curves start converging. From engineering point of view, the values of  $C_2$  equal to 15 m, 20 m or 25 m are equally good as they represent very little difference in the load at the onset of significant nonlinearity.

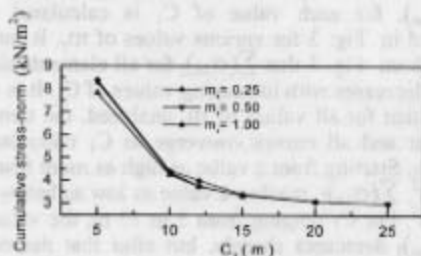


Fig. 5 Variation of cumulative stress-norm along  $BD_2$  with radial distance from pile center.

Figure 5 shows the variation of  $\sum(\sigma_{sn})_i$  for boundary 2 i.e.  $BD_2$  (Fig. 3, Eq. 3) with increasing value of  $C_2$ . As expected, the values of  $\sum(\sigma_{sn})_i$  decreases exponentially with increasing value of  $C_2$ . For values of  $C_2$  between 5 to 15 m, the curves show significant decline, but after that the rate of decrease becomes sluggish and use of a very large value of  $C_2$  (say  $C_2$  equal to 30 m) would result in very little improvement in the load deflection behaviour. From

all these comparative analyses, it can be stated, admittedly tentatively, that the use of  $C_2$  equal to 3/4 H (i.e. 15 m in the present case) may lead to satisfactory prognosis in all cases with  $m_r$  equal to 0.5 or less.

### 4.3 Determination of $m_r$

Till now, three different values for rate of increase of element dimension have been investigated for fixing  $C_1$  and  $C_2$ . This article deals exclusively with the effect of  $m_r$  on the predicted response and a fourth value of  $m_r$  has also been investigated here. Other parameters have been fixed in the light of previous sections and they are presented in Table 8.

Table 8. Parameters used in analysis for fixing  $m_r$

$m_r$ (m/element)	$C_1$ (m)	$C_2$ (m)	$L_i$	$N_1$	$N_2$	$T_1$ (m)
1.0,0.5,0.25 0.125	20	15	$L_1$	20	2	0.05

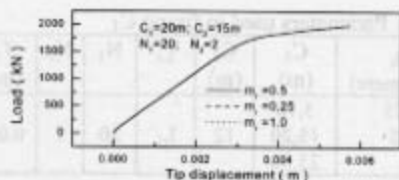


Fig. 6 Load-displacement curves for various  $m_r$ .

Figure 6 shows the effect of varying  $m_r$  on load-displacement curves. It is clear from Fig. 6 that for the three values of  $m_r$  used in this analysis, the load-displacement curves completely converge into one. Since the use of  $m_r$  equal to 1.0 results in too high value of aspect ratio for some elements distant from pile, for satisfactory finite element analysis a value of  $m_r$  equal to 0.5 appears to be reasonable.

### 4.4 Determination of load increment, $L_i$

This analysis uses incremental loading method which makes the selection of proper loading-increment. In the present analysis, six different load-increments are investigated and the load-increments are reduced gradually using the understanding gained from the previous higher load increment analysis. Other parameters used are given in Table 9.

Table 9. Parameters used for fixing  $L_i$  (Fig. 7).

$C_1$ (m)	$C_2$ (m)	$L_i$	$N_1$	$N_2$	$T_1$ (m)
20	15	$L_1, L_2, L_3, L_4$ $L_5, L_6$	20	2	0.05

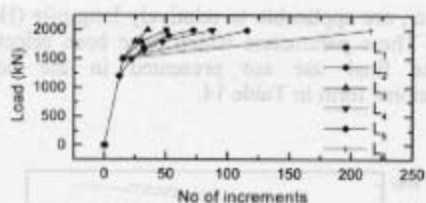


Fig. 7 Load increment rate  $L_1, L_2, L_3, L_4, L_5$  and  $L_6$ .

The load-displacement curves for different load-increment ratios are shown in Fig. 8. It can be stated from the figure that for the linear portion of load-displacement curves the size of load increments do not have any effect. But, as expected, in the non-linear portion of the curves, displacements at the pile tip for any particular load increases with decreasing load-increment sizes. The load-increment rate,  $L_1$  had been used for the all previous analysis.

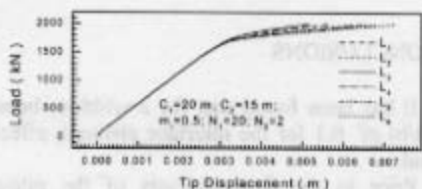


Fig. 8 Load-displacement curves for various loading rates.

If the trend of all curves are observed in Fig. 8, a realistic and reasonably accurate load increment rate can be suggested. For 0 to 1500 kN load, an increment size of 100 is acceptable. Then for 1500 to 1900 load, an increment size of 5 kN and for 1900 to 2000 kN load, an increment size of 2.5 kN can be selected. But if running time is of less importance, then the load-increment rate of  $L_6$  may be used.

#### 4.5 Determination of $N_1$

The size of elements connecting interface elements should be equal as otherwise, it would be difficult, in the present case, to keep the aspect ratio of interface elements within specified limit (Desai et al., 1984). In this analysis, it has been tried to keep the size of elements adjacent to interface elements constant and, subsequently, vertical dimension of all elements within the soil surface and pile tip have been kept constant. Here  $N_1$  is the number of these equal length elements along the pile length.

All other parameters fixed in previous articles and used in this comparative study are presented in Table 11 along with the different values of  $N_1$  used here.

Table 11. Parameters used in the analysis for fixing  $N_1$

$m_r$ (m/element)	$C_1$ (m)	$C_2$ (m)	$L_i$	$N_1$	$N_2$	$T_i$ (m)
0.5	20	15	$L_1$	12,16 20,40	2	0.05

The effect of the variation of  $N_1$  on load-displacement behaviour is investigated and shown in Fig. 9. It can be seen from Fig. 9 that the increase of the number of elements along pile shaft over 20 does not produce any benefit as both the curves for  $N_1$  equal to 20 and 40 almost converge to one. Other lower values of  $N_1$  such as  $N_1$  equal to 16 or 12, produce gradual deviation from the converged group, as expected.

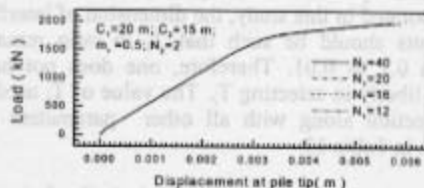


Fig. 9 Load-displacement (tip) curves for various  $N_1$

From all these extensive analyses, it can be concluded that the value of  $N_1$  may be set at 20 (i.e.  $H/2D$  as put in the present case).

#### 4.6 Determination of $N_2$

The radial extent of this high stress zone, for which element dimensions should be smaller, has been fixed at twice the diameter of the pile ( $2D$ ) in any direction from pile tip as shown in Fig. 1. The other parameters used here are presented in Table 12 along with different values of  $N_2$ .

Table 12. Parameters used in analysis for fixing  $N_2$

$m_r$ (m/element)	$C_1$ (m)	$C_2$ (m)	$L_i$	$N_1$	$N_2$	$T_i$ (m)
0.5	20	15	$L_1$	20	2,3,4	0.05

Three different values of  $N_2$  have been investigated in this study. Much larger numbers are not used due to the problem associated with aspect ratio of these elements. Figure 10 shows the effect of varying  $N_2$  on load-displacement behaviour. It can



be seen from the plot that an increase in the value of  $N_2$  predicts more deflections, as expected. The number of elements within 2D distance from pile tip has been selected to be 4 i.e. the dimension of these elements may be taken as equal to  $D/2$ .

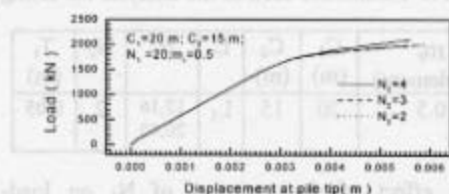


Fig. 10 Load-displacement curves for various  $N_2$

#### 4.7 Determination of $T_i$

The proponents of interface element have prescribed the dimension for these special elements for accurate analysis. For the small thickness interface element proposed by Desai et al. (1984) which has been incorporated in this study, the dimension of interface elements should be such that  $T_i/b$  ratio remains within 0.1 to 0.01. Therefore, one does not have much liberty in selecting  $T_i$ . The value of  $T_i$  used in this section along with all other parameters are shown in Table 13.

Table 13. Parameters used in analysis for fixing up  $T_i$

$m_i$ (m/element)	$C_1$ (m)	$C_2$ (m)	$L_i$	$N_1$	$N_2$	$T_i$ (m)
0.5	20	15	$L_i$	20	4	0.05 0.025 0.0125

The effect of varying interface element thickness on the load-displacement behaviour has been shown in Fig. 11. This load-displacement plot shows that a great deal of deviation of behaviour occurs for  $T_i$  equal to 0.025 and 0.0125 with respect to  $T_i$  equal to 0.05. However, the curves for the value of  $T_i$  equal to 0.025 and 0.0125 almost come together.

Thus, the thickness of interface element may be selected at 0.025 m (which is equal to one tenth of the dimension of adjacent smallest elements). Accordingly, the value of  $T_i$  may be fixed at  $1/10(D/2)$  i.e.  $D/20$ .

## 5 THE FINAL MESH CONFIGURATION

The studies described in the previous sections lead to the selection of mesh configurations, as applicable to piles cast in Dhaka soil. The findings,

however, are applicable to relatively long pile ( $H/D > 20$ ). These parameters which have been selected for the final use are presented in the non-dimensional form in Table 14.

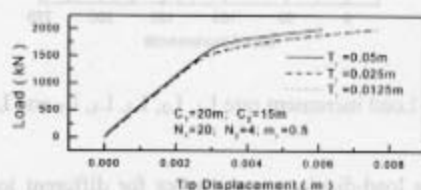


Fig. 11 Load-displacement curves for various  $T_i$

Table 14. Final parameters of mesh configuration.

$m_i$ (m/el.)	$C_1$ (m)	$C_2$ (m)	$L_i$	$N_1$	$N_2$	$T_i$ (m)
D	H	0.75H	$L_i$	$H/(2D)$	4 (D/2)	$(1/10)$ (D/2)

## 6 CONCLUSIONS

1. It has been found that for a width-to-breadth ratio ( $t/b$ ) of 0.1 for the interface element, effect is minimal.
2. Prior to the final analysis of the pile-soil system, the loading rate has to be determined individually for the case concerned.

In this study specific non-dimensional guidelines have been suggested and subsequently tested for obtaining reasonable mesh configurations. The proposed methodology may be suitably adopted to other structure-soil systems.

## REFERENCES

- Bari, M. S. 1996. Development of a Realistic Soil-Structure Interaction System. M.Sc.Engg. Thesis., Civil Engg. Dept. BUET.
- Desai, C. S., Zaman M. M., Lightner, J. G. and Siriwardane, H. J. 1984. Thin-layer Element for Interfaces and Joints, IJNAMG, Vol. 8, pp. 19-43.
- Kamal Uddin, M. 1990. Compressibility and Shear Strength of Remoulded Dhaka Clay. M.Sc.Engg. Thesis., Civil Engg. Dept. BUET.
- Kinoshita, M., Kotsivos, M. D. and Pavlovic, M. N. 1994. Behaviour of Concrete under Passive Confinement, J. Mat., Concr. Struct. & Pavements, Proc. JSCE, Vol. 25, pp. 131-142.
- Siddique, A. and Safiullah, A. M. M. 1995. Permeability Characteristics of Dhaka Clay, J. of the CE Div., IEB, Vol. 23/CE, No.1, pp. 103-116.